SHAPING ACOUSTIC BACK RADIATION OF LOUDSPEAKERS VIA SUBWAVELENGTH CORRUGATED SURFACES

Federico Vescovi[1], Pio F. Calogero[1], Alberto Bernardini[1], Letizia Chisari[2,3], Enrico Ricciardi[3]

[1] *Department of Electronics, Information and Bioengineering, Politecnico di Milano, Italy*
[2] *Department of Engineering and Informatics, University of Sussex, United Kingdom*
[3] *Labirinti Acustici, Via Gian Francesco Pizzi 20, Milano, Italy*

This paper is a revised version of the authors' submitted manuscript that was peer-reviewed by at least two anonymous reviewers.

Abstract

The interaction between the enclosure and the acoustic back radiation generated by a loudspeaker driver plays a crucial role in shaping the overall emission characteristics of the loudspeaker system. In this study, Subwavelength Corrugated Surfaces (SCSs), a class of acoustic metasurfaces, are proposed to passively control the internal propagation of acoustic back radiation and its angular redistribution. The proposed approach enables the refocusing of the back radiation in lateral directions, while preserving an on-axis sound pressure level comparable to that of a conventional closed-box loudspeaker within the frequency range where the metasurface is effective. The behavior of the system is assessed through a numerical investigation based on finite-element modeling in COMSOL Multiphysics. Three configurations are analyzed: a conventional closed-box system, a loudspeaker system with an open side wall, and a system with open side wall incorporating the SCS. The simulations allow a direct comparison between the different solutions and highlight the potential of SCSs to shape loudspeaker acoustic back radiation and extend directivity control through compact, purely passive structural modifications.

Keywords: *loudspeakers, acoustic metamaterials, subwavelength corrugated surfaces, directivity control*

1. Introduction

The acoustic back radiation generated by loudspeaker drivers has long been known to significantly influence the overall emission characteristics of loudspeaker systems through its interaction with the enclosure, as formalized in the early low-frequency electro-acoustic models by Thiele and Small [1], [2].

Corresponding author: *l.chisari@sussex.ac.uk.*

In conventional closed-box configurations, the acoustic back radiation generated by the driver is confined within the enclosure, where it interacts with the internal air volume, which acts as an acoustic compliance. At the same time, the confinement of the rear wave may lead to internal reflections and standing-wave patterns, which can affect spectral smoothness and introduce coloration if not properly controlled.

Traditional mitigation strategies include the use of absorbing materials to damp internal modes and reduce stored acoustic energy. Alternatively, vented alignments (e.g., bass-reflex systems) can be employed, in which the rear radiation is deliberately coupled to an acoustic port and partially re-radiated to enhance low-frequency efficiency and bandwidth [3].

In recent years, acoustic metamaterials and metasurfaces have emerged as a powerful framework for advanced wave manipulation, enabling control over wave propagation that far exceeds what is achievable with traditional materials [4], [5]. These engineered subwavelength structures exploit local resonances, periodicity, and tailored impedance distributions to manipulate the phase, amplitude, and direction of propagating waves. In particular, gradient-index and phase-gradient metasurfaces have demonstrated unprecedented control of acoustic wavefronts through generalized Snell's laws, enabling anomalous reflection, beam steering, and negative refraction [6], [7], [8]. These concepts have inspired a wide range of applications, including cloaking, compact wavefront shaping, sound focusing, and broadband directional control [9], [10].

Within the loudspeaker domain, research on labyrinthine and metamaterial-based approaches has predominantly focused on enhancing sound absorption and damping within the enclosure to mitigate standing waves and internal resonances that degrade spectral smoothness. In [11], the broader potential of acoustic metamaterials in loudspeaker system design is discussed, highlighting the state-of-the-art applications of these engineered structures for advanced

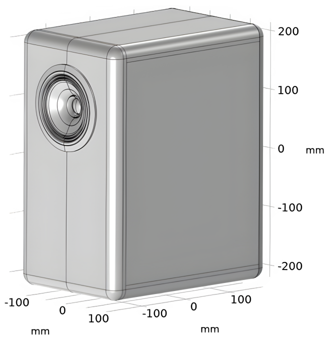

Figure 1: Closed-box loudspeaker system.

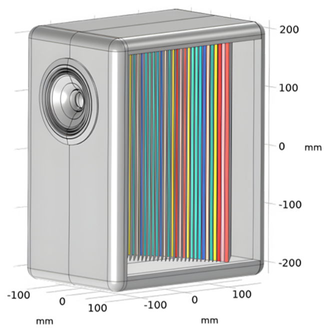

Figure 2: SCS-based system with open lateral side. Different colors of the SCS are used to improve visualization.

sound shaping and directivity control. Degraeve *et al.* [12] demonstrated the application of a metamaterial absorber tailored for loudspeaker enclosures, exploiting deep subwavelength resonant elements to achieve absorption performance beyond what is possible with conventional porous materials and massive dampers alone. Similarly, in [13], preliminary studies on metamaterial-based audio systems show that compact metasurface architectures can be used not only to reduce unwanted emissions but also to shape backward and side emissions with significant system weight reduction. However, despite these advances, the potential of acoustic metasurfaces to shape and redirect acoustic back radiation, rather than simply attenuate it, remains relatively unexplored. This capability could open new directions for directivity control and tailored emission patterns in loudspeaker systems beyond traditional designs.

In this work, we focus on Subwavelength Corrugated Surfaces (SCSs), a specialized class of metamaterials formed by arrays of subwavelength grooves or corrugations that impose spatially varying phase delays on reflected waves through geometric modulation, enabling precise control of the local phase response [14], [15], [16], [17], [18], [19]. By properly designing the depth and arrangement of these corrugations, SCSs allow compact, purely passive control of wavefront direction, focus, and reflection characteristics over relatively broad bandwidths. Such structures have been shown, both theoretically and experimentally, to support dispersionless manipulation of acoustic wavefronts, including extraordinary reflection angles and broadband steering, demonstrating their potential for advanced acoustic wave shaping [20].

The objective of this study is to harness the backward radiation of a loudspeaker driver to extend horizontal coverage and modify system directivity without compromising the on-axis response. By integrating an SCS within a partially open enclosure, a controlled phase profile is imposed on the rear wave, redirecting it toward a prescribed lateral direction by using planar focusing. The proposed SCS-based approach is compared through finite-element simulations in COMSOL Multiphysics with conventional closed-box and partially open configurations, in terms of radiation pattern, spectral balance, and angular redistribution.

2. SCS-Based Loudspeaker System

2.1. Proposed System Structure

The proposed loudspeaker system evolves from a conventional closed-box configuration consisting of a cabinet and a single driver, as depicted in Fig. 1. In the reference case, the driver's backward radiation is entirely confined within the enclosure, where it primarily contributes to the internal pressure loading without participating in the external sound field. In the modified architecture, one lateral wall of the cabinet is removed, thereby creating an open side that acts as an additional radiation aperture. To passively control the otherwise trapped rear emission, a SCS is integrated inside the enclosure, replacing the original rear wall. The SCS matches the height and width of the cabinet back panel and is engineered to impose a spatially varying reflection phase distribution. This phase profile enables planar focusing of the backward-radiated acoustic field toward the open lateral side. The resulting SCS-based configuration is shown in Fig. 2.

The proposed solution is shown in Fig.3. The imposed phase gradient produces a hyperboloidal reflected wavefront, characterized by a double-cone behavior: the reflected field first converges toward a prescribed focal point and subsequently diverges toward the lateral opening. The focal point is positioned along the boundary of the removed wall, approximately at the mid-width of the aperture, ensuring that the reflected energy is preferentially redirected toward the opening and efficiently re-emitted in the horizontal plane.

To enhance angular robustness, the SCS is rotated 45° with respect to the original rear-wall orientation. This configuration promotes a more symmetric double-cone distribution and mitigates sensitivity to the range of incident angles associated with the back radiation of the driver.

Overall, the enclosure retains the compact form factor of a conventional closed-box system while introducing a controlled lateral radiation component achieved through purely passive geometric wavefront shaping.

2.2. On the design of the SCS

The backward radiation of the driver is modeled as a plane wave propagating toward the rear wall of the

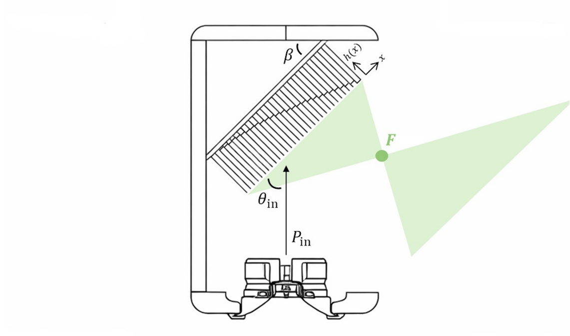

Figure 3: Scheme of the proposed solution.

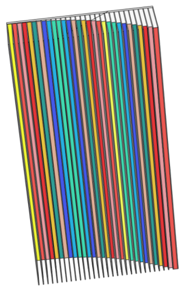

Figure 4: Designed SCS.

enclosure along the direction orthogonal to it. Due to the rotation with angle $\beta = \pi/4$ of the SCS with respect to the cabinet rear wall, this wave impinges on the corrugated surface with an oblique incidence angle $\theta_{\text{in}} = \pi/2 - \beta$.

The continuous groove-depth function of the SCS is expressed as [20]

$$h(x) = C - \frac{1}{2k_0}\phi(x) \tag{1}$$

where C is a constant introduced to ensure that $h(x)$ remains positive, $k_0 = 2\pi/\lambda$ is the wavenumber, λ is the acoustic wavelength, and $\phi(x)$ is the prescribed spatial phase profile.

The phase profile is designed such that the term $\phi(x)/(2k_0)$ is independent of wavelength, resulting in a dispersionless reflected wavefront. To focus sound at an arbitrary point $F_0 = (x_0, y_0)$, the hyperboloidal phase profile proposed in [20] is generalized here by accounting for an incident plane wave arriving from an arbitrary direction, defined in this work as $\theta_{\text{in}} = \pi/2 - \beta$. The resulting expression is

$$\phi(x) = k_0 \left(x \sin\beta + \sqrt{(x - x_0)^2 + y_0^2} - \sqrt{x_0^2 + y_0^2} \right) \tag{2}$$

which reduces to Eq. (12) in [20] when $\beta = 0$, i.e., when the incident wavefront of the plane wave reaches all grooves with identical phase.

In the practical implementation of the SCS, the continuous function $h(x)$ is spatially sampled to generate a finite number N of grooves. The groove period d and the groove width d_0 are selected according to the subwavelength design criteria discussed in [20]. The designed SCS is shown in Fig. 4.

3. Numerical Validation

To evaluate the impact of the SCS on the acoustic performance of the system, three configurations are analyzed: a conventional closed-box loudspeaker, with internal and external cabinet dimensions, i.e, 350 × 238 × 434 mm and 304 × 199 × 380 mm, respectively, a partially open cabinet obtained by removing one lateral wall, and the proposed solution characterized by the same partially open cabinet integrating the SCS.

All simulations are carried out in COMSOL Multiphysics in the frequency range from 100 Hz to 6.3 kHz consistent with ISO frequencies in third-octave band subdivision. The selected range reflects the effective operating bandwidth of the SCS, excluding frequencies where subwavelength phase control is not expected to be effective [20]. The computational domain is enclosed by a spherical Perfectly Matched Layer (PML) with a radius of 360 mm, ensuring absorption of outgoing waves and minimizing reflections. A consistent mesh resolution is adopted across all configurations, with a maximum element size equal to $\lambda/4$ throughout the domain. The loudspeaker is modeled using an electro-mechano-acoustic representation of the SICA 5.5C1.5CP-8 driver, excited by a peak voltage of 4 V. The simulations employ a hybrid mesh composed of triangular and tetrahedral elements and consider exclusively the acoustic radiation of the woofer, neglecting the tweeter contribution.

3.1. Closed-Box System

The enclosure of the closed-box loudspeaker system is modeled with perfectly rigid walls to emphasize the ideal radiation behavior and to reduce computational complexity.

The on-axis frequency response, evaluated at a distance of 1 m from the loudspeaker, is represented by the blue line in Fig. 11. It exhibits a pronounced peak around 2 kHz, followed by attenuation at both lower and higher frequencies. Deviations from the typical low-frequency behavior of a woofer are observed below 200 Hz, primarily due to the limited absorption performance of the PML for long wavelengths within the finite computational domain in COMSOL.

Fig. 5 shows the horizontal directivity map of the system, computed with respect to the geometric center of the driver and evaluated along a circular path of radius 1 m. Maximum sound pressure levels occur along the frontal axis (0°), with a progressive decay toward ±180°. The directivity becomes increasingly pronounced with frequency, in agreement with the expected behavior of conventional closed-box loudspeakers.

A cross-sectional view of the acoustic field distribution at 4 kHz is reported in Fig. 6.

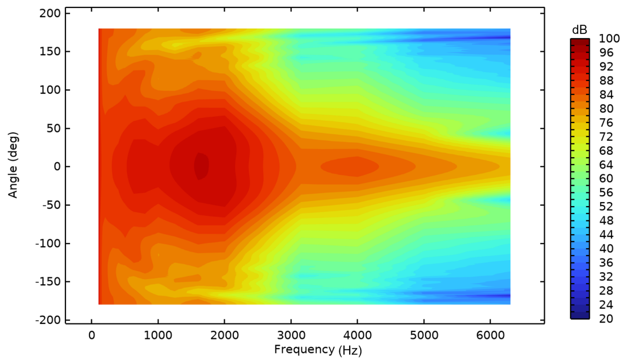

Figure 5: Horizontal directivity map of the closed-box configuration measured at 1 m.

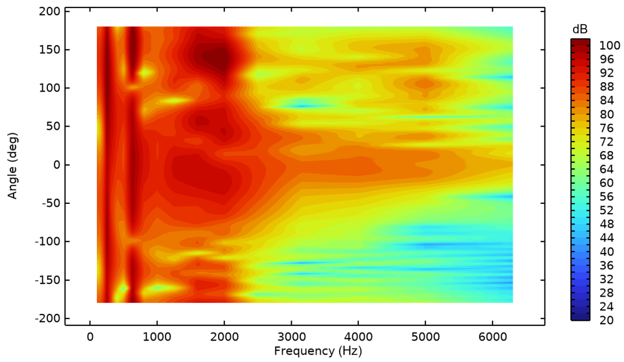

Figure 7: Horizontal directivity map of the configuration with an open side wall measured at 1 m.

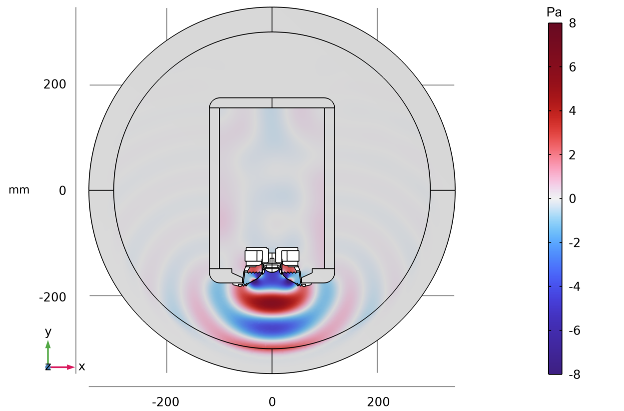

Figure 6: Acoustic pressure distribution at 4 kHz on the $z = 0$ plane for the closed-box configuration.

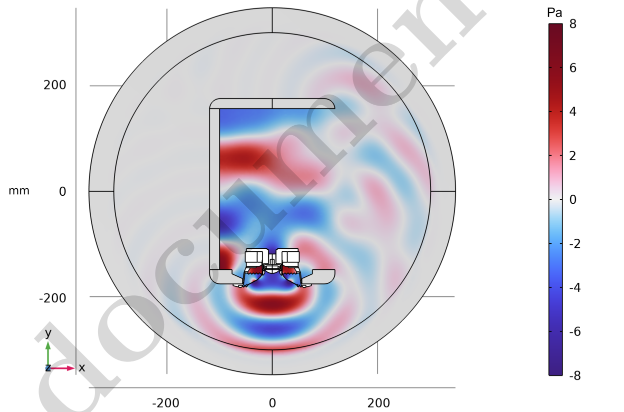

Figure 8: Acoustic pressure distribution at 4 kHz on the $z = 0$ plane for the open side-wall configuration.

3.2. Partially Open System

The second configuration features the same cabinet geometry with one lateral wall removed. This setup serves as an intermediate reference case, isolating the effect of the lateral opening prior to the integration of the SCS.

The on-axis frequency response evaluated at 1 m, represented by the green line in Fig. 11, exhibits pronounced oscillations across the analyzed frequency range. Compared to the closed-box configuration, the response is significantly more irregular. This behavior arises from the release of acoustic energy that, in the sealed enclosure, remains confined and is now allowed to radiate through the lateral opening.

In the absence of a phase-control mechanism, the backward radiation interacts with the forward field introducing interference effects that alter the spectral response. In addition, strong internal reflections between the front and rear walls persist, while cavity resonances are no longer fully confined, further contributing to the observed response irregularities.

The horizontal directivity map of the partially open system in Fig. 7 shows a pattern broadly similar to that of the closed-box configuration, with the addition of lateral radiation components between 0° and 180°. These components result from the uncontrolled back radiation escaping through the opening, as illustrated in Fig. 8.

Although the lateral dispersion increases on the open side, the associated spectral irregularities indicate that the simple removal of the lateral wall fails to provide controlled directivity extension and does not constitute a viable solution in practical terms.

3.3. Proposed SCS-based System

The proposed configuration is obtained by integrating the designed SCS into the partially open cabinet described in Section 3.2. The SCS is engineered to reflect the backward-radiated acoustic field toward a prescribed focal region, as illustrated in Fig. 9. The focal point, indicated by a green marker in Fig. 9, is positioned along the boundary at the mid-width of the removed lateral wall to minimize internal reflections while promoting lateral emission. The resulting radiation pattern arises from both the wavefronts shaped by the SCS and the portion of back radiation that is not intercepted by the corrugated surface.

The implemented SCS has overall dimensions of 380 mm (height), 202 mm (width), and 75 mm (depth). The structure consists of $N = 30$ corrugations with a spatial period of $d = 6.7$ mm, groove width of $d_0 = 5.7$ mm and groove depths ranging from 0 to 69 mm. A three-dimensional representation of the

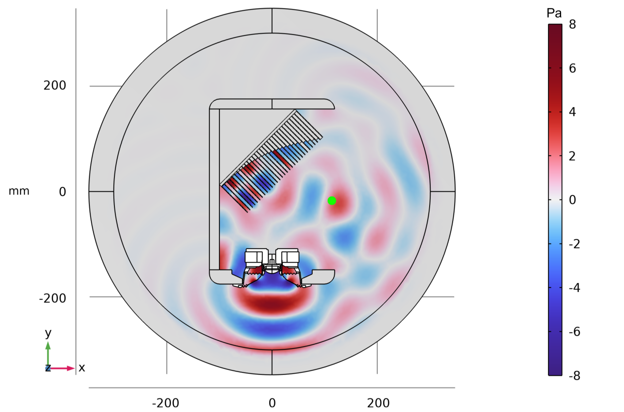

Figure 9: Acoustic pressure field at 4 kHz on the $z = 0$ plane for the focusing SCS configuration. The green dot indicates the position of the acoustic focal point.

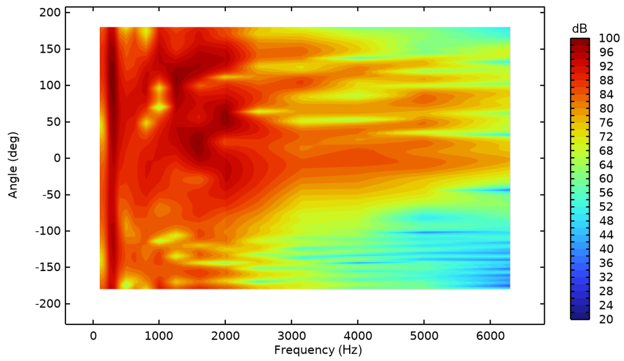

Figure 10: Horizontal directivity pattern of the configuration with SCS measured at 1 m from the loudspeaker center.

designed geometry is shown in Fig. 4.

The on-axis frequency response, represented by the yellow line in Fig. 11, exhibits a behavior intermediate between closed-box and partially open configurations. Although resonance peaks remain present, the overall spectral trend is more regular than in the open-wall configuration, exhibiting a frequency response that closely aligns with that of the closed-box system above 500 Hz.

The horizontal directivity map shown in Fig. 10 confirms the achievement of enhanced lateral emission on the open side of the system. Compared with the partially open configuration shown in Fig. 7, the radiation pattern is slightly more concentrated, showing a clearer separation between frontal emission and deflected back radiation. Moderate attenuation around 180° is also observed, consistent with the intended lateral redirection of acoustic energy.

Overall, the SCS-based configuration preserves the lateral dispersion introduced by the opening while providing improved control over the backward radiation, although the quantitative improvements with respect to the open configuration remain limited within the analyzed frequency range.

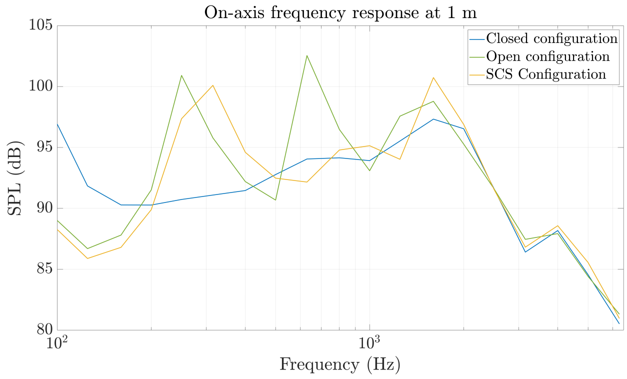

Figure 11: Comparison of the frequency responses measured on-axis at 1 m for the three analyzed configurations.

4. Conclusions and Future Works

A comprehensive comparison of the analyzed configurations highlights a clear trade-off between on-axis spectral smoothness and extended horizontal directivity. The closed-box system ensures the most uniform on-axis frequency response across the investigated bandwidth. However, it does not provide any mechanism for lateral energy redistribution. In contrast, the partially open configuration promotes lateral radiation, but this at the expense of introducing pronounced spectral irregularities, arising from uncontrolled back radiation and internal interference phenomena.

By introducing the SCS, the backward-radiated field is intentionally redirected toward the lateral aperture, partially mitigating the interference mechanisms observed in the open wall case. Above approximately 500 Hz, the frontal response becomes noticeably smoother than in the partially open configuration, indicating a reduced interference between forward radiation and the acoustic field escaping through the opening. This behavior reflects improved phase control of the reflected field.

At lower frequencies, the observed performance degradation is consistent with the inherent limitations of subwavelength corrugated structures, whose phase-control effectiveness progressively decreases as the acoustic wavelength becomes significantly larger than the groove width. Conversely, beyond approximately 1 kHz, the SCS exerts a more efficient wavefront-shaping action, reducing uncontrolled reflections and stabilizing the frontal spectral response while preserving lateral emission.

Overall, the proposed approach demonstrates that backward radiation can be exploited as a controllable acoustic resource through passive geometric shaping, without the need for additional radiating elements. Although the quantitative improvements remain limited, the results confirm the feasibility of extending the directivity angle through engineered redirection of the rear acoustic field.

Future developments will explore alternative open-enclosure configurations incorporating single or multiple SCSs elements to further enhance lateral energy redistribution while preserving frontal spectral smoothness. In particular, arrays of SCS metasurfaces with varying orientations may enable more advanced radiation pattern synthesis and broader-band control of the backward-radiated field. Experimental validation using physical loudspeaker prototypes will be carried out to evaluate the practical implementation of the concept and to quantify the influence of structural vibrations, material damping, and manufacturing tolerances. Additional optimization of the SCS geometry will also be pursued to achieve broader bandwidth performance and improved low-frequency performance, where subwavelength phase control remains intrinsically constrained.

References

[1] A. N. Thiele, "Loudspeakers in vented boxes: Part i," *Journal of the Audio Engineering Society*, vol. 19, no. 5, pp. 382–392, 1971.

[2] R. H. Small, "Direct-radiator loudspeaker system analysis," *Journal of the Audio Engineering Society*, vol. 20, no. 5, pp. 383–395, 1972.

[3] R. Balistreri, "An improved loudspeaker frequency response by using a structure of rigid absorptive panel in a vented cabinet," in *Proceedings of the 2014 COMSOL Conference*, Boston, USA, Oct. 2014.

[4] D. Lee, D. M. Nguyen, and J. Rho, "Acoustic wave science realized by metamaterials," *Nano Convergence*, vol. 4, no. 1, p. 3, 2017.

[5] M. Yang and P. Sheng, "Sound absorption structures: From porous media to acoustic metamaterials," *Annual Review of Materials Research*, vol. 47, no. 1, pp. 83–114, 2017.

[6] S. Sun, Q. He, S. Xiao, Q. Xu, X. Li, and L. Zhou, "Gradient-index meta-surfaces as a bridge linking propagating waves and surface waves," *Nature Materials*, vol. 11, no. 5, pp. 426–431, 2012.

[7] Y. Xie, W. Wang, H. Chen, A. Konneker, B.-I. Popa, and S. A. Cummer, "Wavefront modulation and subwavelength diffractive acoustics with an acoustic metasurface," *Nature Communications*, vol. 5, no. 5553, pp. 1–8, 2014.

[8] J. Li, A. Song, and S. A. Cummer, "Bianisotropic acoustic metasurface for surface-wave-enhanced wavefront transformation," *Physical Review Applied*, vol. 14, no. 4, p. 044 033, 2020.

[9] Y. Li, X. Jiang, R. Li, B. Liang, X. Zou, L. Yin, and J. Cheng, "Experimental realization of full control of reflected waves with subwavelength acoustic metasurfaces," *Phys. Rev. Appl.*, vol. 2, no. 6, p. 064 002, 2014.

[10] Y. Li, B. Liang, Z. Gu, X. Zou, and J. Cheng, "Reflected wavefront manipulation based on ultrathin planar acoustic metasurfaces," *Scientific Reports*, vol. 3, no. 1, p. 2546, 2013.

[11] L. Chisari, M. D. Cola, and P. Martignon, "Acoustic metamaterial in loudspeaker systems design," in *Proc. of the Audio Engineering Society 2019 Convention*, New York, USA, 2019, PD18–PD18.

[12] S. Degraeve and J. Oclee-Brown, "Metamaterial absorber for loudspeaker enclosures," in *Proc. of the 148th Audio Engineering Society International Convention*, Online, 2020, pp. 1–9.

[13] L. Chisari, M. D. Cola, P. Martignon, and G. Memoli, "Preliminary studies for metamaterial-based audio systems," in *Proc. of the European Acoustics Association Euronoise*, Madeira, Portugal, 2021.

[14] R. Lipton, A. Polizzi, and L. Thakur, "Novel metamaterial surfaces from perfectly conducting subwavelength corrugations," *SIAM Journal on Applied Mathematics*, vol. 77, no. 4, pp. 1316–1339, 2017.

[15] J.-J. Wu, "Subwavelength microwave guiding by periodically corrugated strip line," *Progress In Electromagnetics Research*, vol. 103, no. 1, pp. 307–322, 2010.

[16] B. G. Cai, Y. B. Li, H. F. Ma, W. X. Jiang, Q. Cheng, and T. J. Cui, "Leaky-wave radiations by modulating surface impedance on subwavelength corrugated metal structures," *Scientific Reports*, vol. 6, no. 1, p. 22 060, 2016.

[17] M. Beruete, M. Sorolla, I. Campillo, and J. S. Dolado, "Subwavelength slotted corrugated plate with enhanced quasioptical millimeter wave transmission," *IEEE Microwave and Wireless Components Letters*, vol. 15, no. 4, pp. 286–288, 2005.

[18] V. I. Shcherbinin, V. I. Fesenko, T. I. Tkachova, and V. R. Tuz, "Superscattering from subwavelength corrugated cylinders," *Physical Review Applied*, vol. 13, no. 2, p. 024 014, 2020.

[19] M. W. B. Silva and L. C. Kretly, "A new concept of ram-radiation absorbent material: Applying corrugated surfaces to improve reflectivity," in *Proc. of the 2011 SBMO/IEEE MTT-S International Microwave and Optoelectronics Conference*, Natal, Brazil, 2011, pp. 1–4.

[20] Y.-F. Zhu, X.-Y. Zou, R.-Q. Li, X. Jiang, J. Tu, B. Liang, and J.-C. Cheng, "Dispersionless manipulation of reflected acoustic wavefront by subwavelength corrugated surface," *Scientific Reports*, vol. 5, no. 10966, pp. 1–10, 2015.